Ministry of National Infrastructures
Geological Survey of Israel

Modeling the relation between area and volume of landslides

Boriana Kalderon-Asael, Oded Katz, Einat Aharonov, Shmuel Marco

Submitted to the Steering Committee for Preparation for Earthquakes

Jerusalem, April 2008 Report GSI/06/2008

Ministry of National Infrastructures

Geological Survey of Israel

Modeling the relation between area and volume of landslides

Boriana Kalderon-Asael[1,2], Oded Katz[1], Einat Aharonov[3], Shmuel Marco[2]

1. Geological Survey of Isreal, Jerusalem.
2. Dept. of Geophysics and Planetary Sciences, Tel Aviv University.
3. The Institute of Earth Sciences, The Hebrew University, Jerusalem.

Submitted to the Steering Committee for Preparation for Earthquakes

Jerusalem, April 2008 Report GSI/06/2008

Abstract

A remarkable observation in real landslides is that landslides of different sizes, from different locations around the globe, triggered by different mechanisms, all seem to have scale-independent shapes, with their volume to surface area ratio following a power law. The physical basis for this observation is poorly understood.

In the presented work we model (using a slope-stability computer program) the relation between surface area and volume of landslides in homogenous slopes. We establish, based on the computer simulations, a universal relationship between volume (V) and area (A) of landslides. This relationship follows a power law ($V \sim A^{1.4}$) independent of slope height and mechanical properties. The power law has a similar exponent as that for the distribution of both natural subaerial and submarine landslides. The model and field observations suggest that landslide shapes follow a self-affine (not self similar) behavior, with Hurst exponent of 0.74, i.e. as the area of landslides increases they become relatively shallow.

These findings have important implication for hazard analysis. It can be applied to estimate the expected volume of a landslide, given the soil thickness or potential failure plane and to estimates the hazard of landslide-generated tsunamis.

Table of Contents

1. Introduction

A remarkable observation in real landslides is that landslides of different sizes, from different locations, triggered by different mechanisms, all seem to have scale independent shapes, with their surface area (A) to volume (V) ratios following a single power law. Figure 1 presents on a single plot eight reported observations, each compiled from up to a few hundred field measurements (Simonett, 1967; Whitehouse 1983, 1986.; Hovius et al., 1997; Hewitt 2002; Korup 2006; ten Brink et al., 2006; Guzzetti et al., 2008). It can be seen that all the data falls on a single power-law trend, for which $V \sim A^{1.4}$. The data presented comes from widely diverse locations and slope failure processes as detailed in Figure 1. Despite the diversity of origins and mechanisms the different data sets consistently follow a single A to V relation. The physical basis for this observation is poorly understood, but its implications are vast. Such a trend means that landslides are intrinsically scale independent, similar to fractures (Scholz, 2002), i.e., they retain a geometric similarity independent of the scale in which they occur.

We first provide an approximate prediction for geometrical scaling of landslides. In a homogeneous slope the only length scale of the problem is the slope size, H, upon which the slide occurs (Fig. 2). In the absence of any other length scale, simple scaling predicts that the landslide thickness, t, should scale with its lateral dimension, $\sqrt{A}$ (l in our model, see below), and both will scale with H. Thus the landslide volume V, which scales as $t \times A$, is expected to scale as $A^{1.5}$. This simple scaling argument diverges slightly from the $V \sim A^{1.4}$ scaling observed in Figure 1. Our aim is to understand the mechanics controlling scaling of landslide geometry in both homogeneous and heterogeneous environments. The first step in understanding this basic question is to study scaling in homogeneous slopes, although the applicability of the homogeneity hypothesis is not obvious in all natural environments (some of which are highly heterogeneous in terms of their mechanical properties). To this end, we use a simple mechanically based computer model to predict slope failure, and analyze the relation between surface area (A) and volume (V) of landslides in homogenous slopes. Our model results show excellent agreement with the scaling found in field data. The next step, study of failure in heterogeneous slopes, will be presented in a future study.

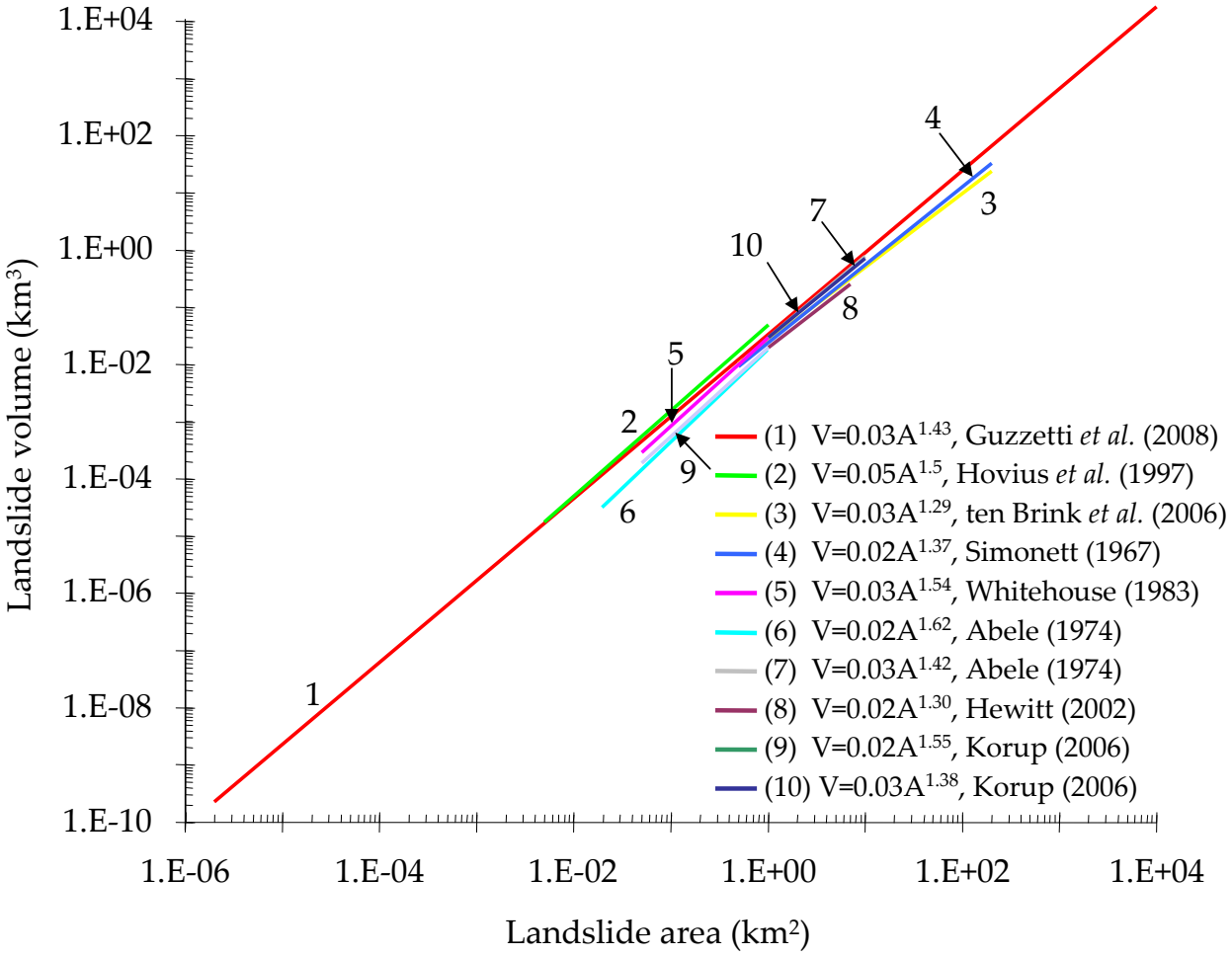

Figure 1. Volume vs. area of worldwide landslide inventories. (1) Compiled inventory of 529 worldwide slides (Guzzetti et al., 2008); (2) 4984 mapped landslides (falls, slumps, slides, and debris flows), representing 60 years of recorded mass wasting from the Montane zone, Western Southern Alps of New Zealand (Hovius et al., 1997); (3) 156 submarine failure scarps (slumps, rock slides, and debris avalanches) along the edge of the carbonate platform in Puerto Rico (ten Brink et al., 2006); (4) 201 landslides in the mountains of New Guinea (Simonett, 1967); (5) deep-seated bedrock landslides in the Central Southern Alps of New Zealand, many of which were controlled by dip-slope schistosity or planes of structural weakness (Whitehouse 1983, 1986); (6) and (7) deep-seated bedrock landslides in the European Alps, whose minimum area is 0.02 km^2 and 1 km^2, respectively (Abele 1974); (8) giant deep-seated landslides in High Asia (Hewitt 2002); (9) and (10) a total of 333 large deep-seated landslides, Southern Alps of New Zealand, whose minimum area is 0.05 km^2 and 1 km^2, respectively (Korup 2006).

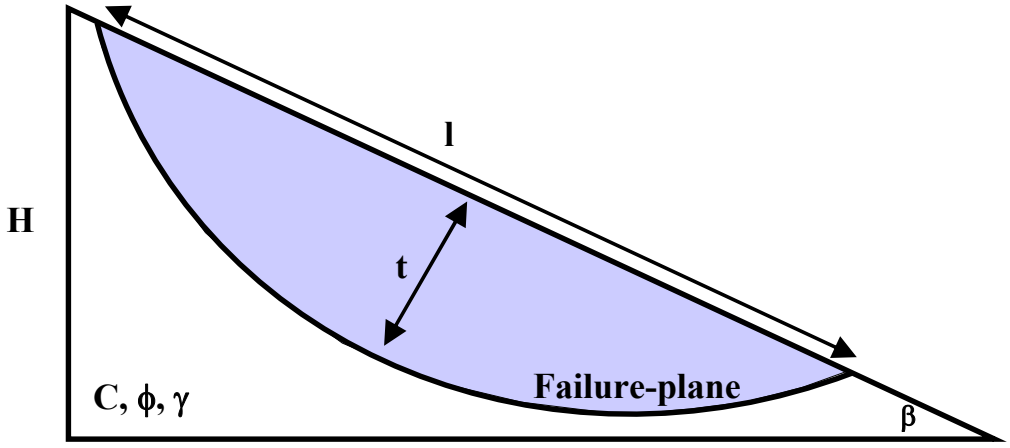

Figure 2. 2D schematic cross section of a landslide (of thickness t and surface length l), originating from a slope of height H and slope angle β. This is the configuration used in our model .

2. Methods

We modeled the expected landslide geometry in a homogeneous slope using the slope stability commercial program SLOPE/W (Geo-Slope Inc.). The modeled slope has a basic triangular shape with a slope angle β. We used β = 26.57°, i.e., a 2:1 ratio of slope's height, H, to base (Fig. 2). The program attempts different circular failure planes (using Bishop, 1955, Simplified Method) and finds the one that is most prone to failure, i.e., the one with the calculated minimal Factor of Safety (FS, the ratio between resisting and driving forces and moments). We tested the dependence of the landslide geometry, characterized by its thickness, t, and its surface length, l, on the slope mechanical properties and geometry. Figure 2 shows our model configuration and a characteristic failure plane. The model simulations were run with varying cohesion (c), angle of internal friction (ϕ), slope height (H) and unit weight (γ) (Table 1).

Table 1: Summary of 100 tested simulated conditions (in all simulations reported here the slope angle is 26.57° and unit weight is 18 kN/m^3)

Slope height, H (m)	Cohesion, c (kPa)	Friction angle, ϕ (deg.)
1,10,100,1000	0,1,2,3,4,5,10,15,20	10, 25
1,10,100,1000	5	3,5,10,15,20,25,30,35,40

Reported here (Table 1) are 100 individual simulations performed under the above described slope angle, unit weight, γ, of 18 kN/m^3, various slope heights, H (1, 10, 100, 1000 m), cohesion, c (0 - 20 kPa) and of friction angle ϕ (3° - 40°), simulating natural mechanical properties of soil and unconsolidated geological material (results using larger unit weight values are similar).

3. Results

3.1. Model results

Each run of the model predicts a landslide with a specific geometry. The landslide geometry for different mechanical conditions used in the model, expressed in terms of resulting thickness, t, and surface length, l (for the case of H=100), is summarized in Figure 3. The model results show that t varies with mechanical properties. It decreases

with decreasing c and with increasing ϕ and spans 1/3 of an order of magnitude. l is practically constant in the studied range of mechanical properties (10% variation), and only sharply decreases or increases close to the limits when either c or ϕ is close to zero, respectively. There are two limiting behaviors to the observed geometry of landslides (Fig. 3): (I) if c = 0kPa and ϕ > 0°, then t → 0 (i.e., very shallow landslide) and (II) if c > 0kPa and ϕ → 0°, then t → maximum (i.e., deepest possible landslide). However, the case of ϕ → 0 does not represent natural geological material. Although the case of c = 0 kPa might represent a natural material (e.g., dry sand) it forms flows and not slumps as the typical slope-failure type. Therefore, we omitted these two cases from the analysis.

For studying the scale effect on landslide sizes, we analyzed 68 simulations (out of the above 100) with H ranging between a meter and a kilometer. In 32 simulations the friction angle was kept constant at 25°, and the cohesion varied (1, 2, 3, 4, 5, 10, 15, 20 kPa) while in another 36 simulations the cohesion was kept constant at 5 kPa, while the friction angle varied (3°, 5°, 10°, 15°, 20°, 25°, 30°, 35°, 40°). We found that the landslide length (l) scales with H ($l \sim H^{\sim 1}$, see Fig. 4), while the landslide thickness (t) increases non-linearly with H ($t \sim H^{0.74}$). As a consequence, the ratio between the landslide thickness, t, and surface length, l (ε, see below), decreases with increasing H. The mechanical properties affect t and l, but do not significantly change their overall scaling with H (Fig. 4).

3.2. Volume-area relations

The model provides a 2D prediction of a failure, but in order to compare to natural field-observed landslides, it is necessary to extrapolate the model results to 3D. The 2D sector of a circle representing the landslide in our model can be transformed into a cap of a sphere that represents the landslide in 3D. Thus, using l, the landslide surface length scale (which in 3D would be the diameter of the cap) and the landslide thickness (t), it is easy to calculate the volume of the correlating 3D landslide cap (V_{cap}) and its surface area (A), according to the following geometrical relations:

$$A = \pi\left(\frac{l}{2}\right)^2 \qquad (1)$$

$$V_{cap} = \frac{1}{6}\pi t\left(3\left(\frac{l}{2}\right)^2 + t^2\right) \qquad (2)$$

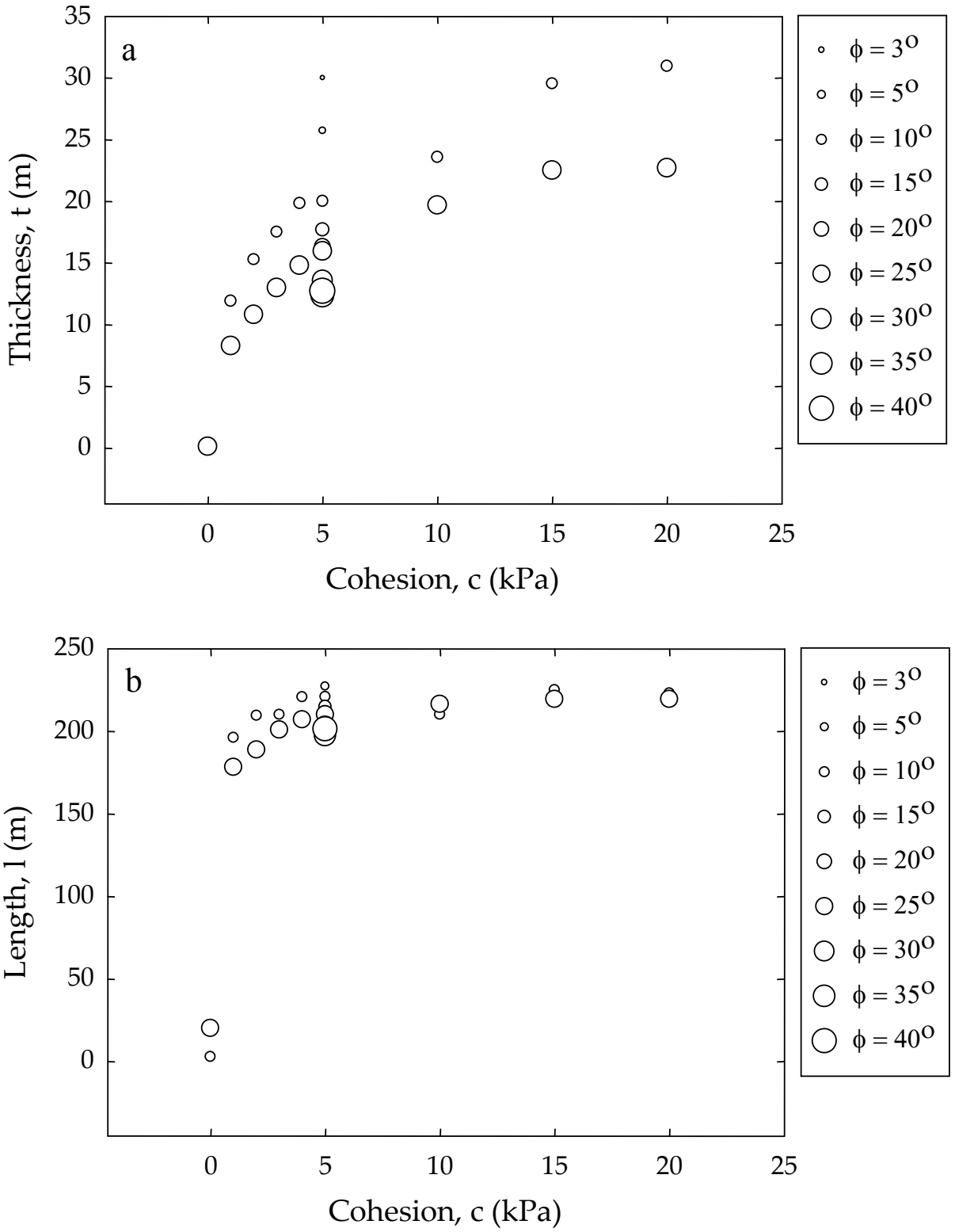

Figure 3. Model predicted landslide geometry (thickness and length) as a function of mechanical properties (cohesion and angle of internal friction). The slope height, H, is 100 m and unit weight ,g, is 18 kN/m^3. (a) landslide thickness, t; (b) landslide length, l .

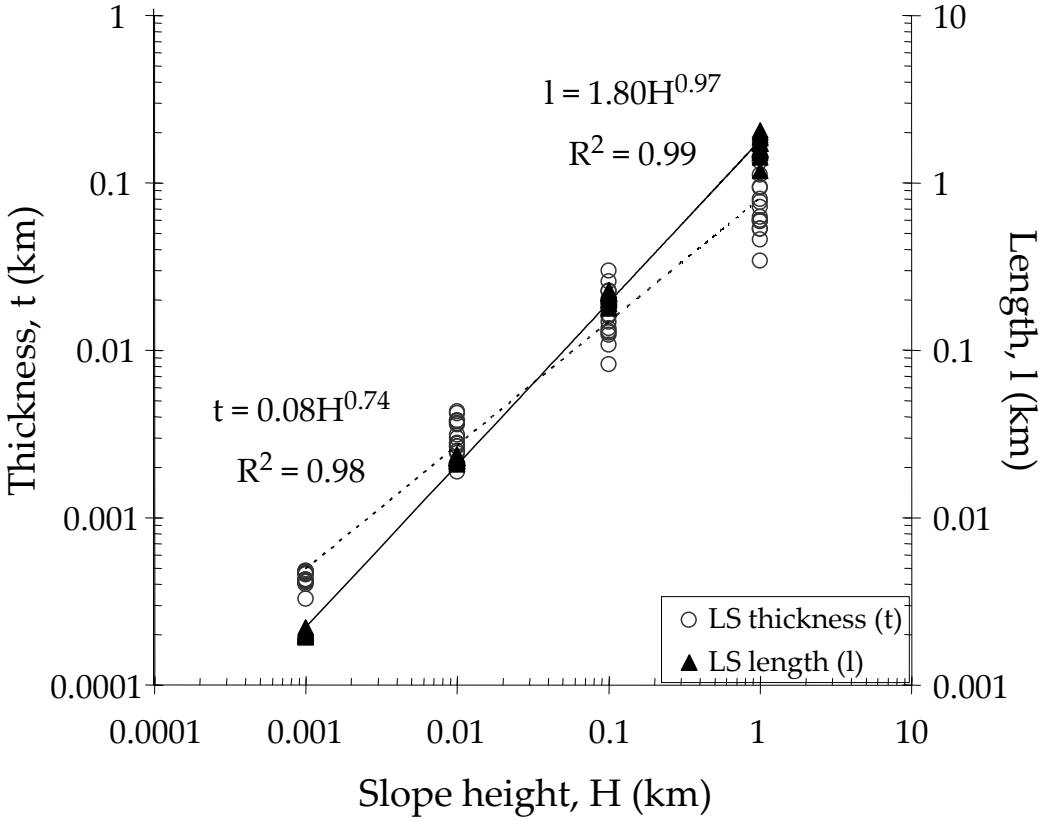

Figure 4 .Model predicted variations of landslide thickness (t, open circles) and landslide length (l, closed triangles) with slope height, H. Plotted are 68 model results obtained with fixed unit weight (γ = 18kN/m^3), fixed slope angle (β = 26.57°) and changing slope height (H=1, 10, 100, 1000m); 32 of the simulations were performed at constant friction angle) ϕ = 25°) and changing cohesion (c = 1, 2, 3, 4, 5, 10, 15, 20 kPa), and the other 36 simulations were performed at constant cohesion (c=5 kPa) and changing friction angle (ϕ = 3, 5, 10, 15, 20, 25, 30, 35, 40°).

The model 2D simulation results, using different slope heights, H, different angle of internal friction, ϕ, and different cohesion, c, produced potential slope failure planes with a range of l and t, as specified in Figure 3. From these 2D results, the predicted 3D volume and area were calculated using Equations 1 and 2. The calculated 3D results follow a universal volume-area relation: $V \sim aA^b$, where a = 0.03±0.01 and b =1.38±0.01 (Fig. 5; for clarity only four trend lines are shown in the figure, however a and b are obtained considering all cases tested in our simulations, not only the four trend lines appearing in the figure).

Alternatively, it is possible to calculate the V to A relation in our modeling results directly from Figure 4, using the fact that $t = 0.08\ H^{0.74}$ and $l = 1.80\ H^{0.97}$. This is done using Eq. 1, to show that $A = 2.54H^{1.94}$, and then using Eq. 2 (and the fact that $t \ll l$, as shown in Fig. 4 and $V=aA^b$) to predict that $V = 0.03A^{1.38}$.

4. Discussion

This section analyzes how our model results contribute to the understanding of the mechanical behavior of natural landslides and to the evaluation of landslide hazard, the question addressed in this manuscript is the source for the amazingly coherent volume (V) to area (A) power-law relations observed in natural landslides (Fig 1). We use a very simple 2D engineering model to look at slope stability of a homogeneous slope of different slope sizes and different mechanical properties. The model finds the most probable failure plane assuming a single circular failure, as shown Figure 2. Model results obtained in 2D were analytically converted to 3D. It was found that even this very simple geotechnical model produces failure planes with volumes and areas that follow a trend very similar to those of field-observations: $V = aA^b$, with a = 0.03±0.01 and b =1.38±0.01, regardless of the cohesive and frictional properties used in the modeling (Fig. 5). Thus, we suggest that the landslide volume-area relation is universal, with $V \sim A^{1.4}$, and is the result of fundamental mechanical and geometrical principles. We are not able at this stage to predict this V-A relationship analytically, but the source of this universal behavior can be discussed from basic principles. There are two questions involved:

1. A self-similar scaling argument would predict that both the slide length l and its thickness t will scale with the slope height H, the only length scale in the problem. In this case $A \sim l^2 \sim H^2$, and $t \sim H$, thus one would predict that V ~

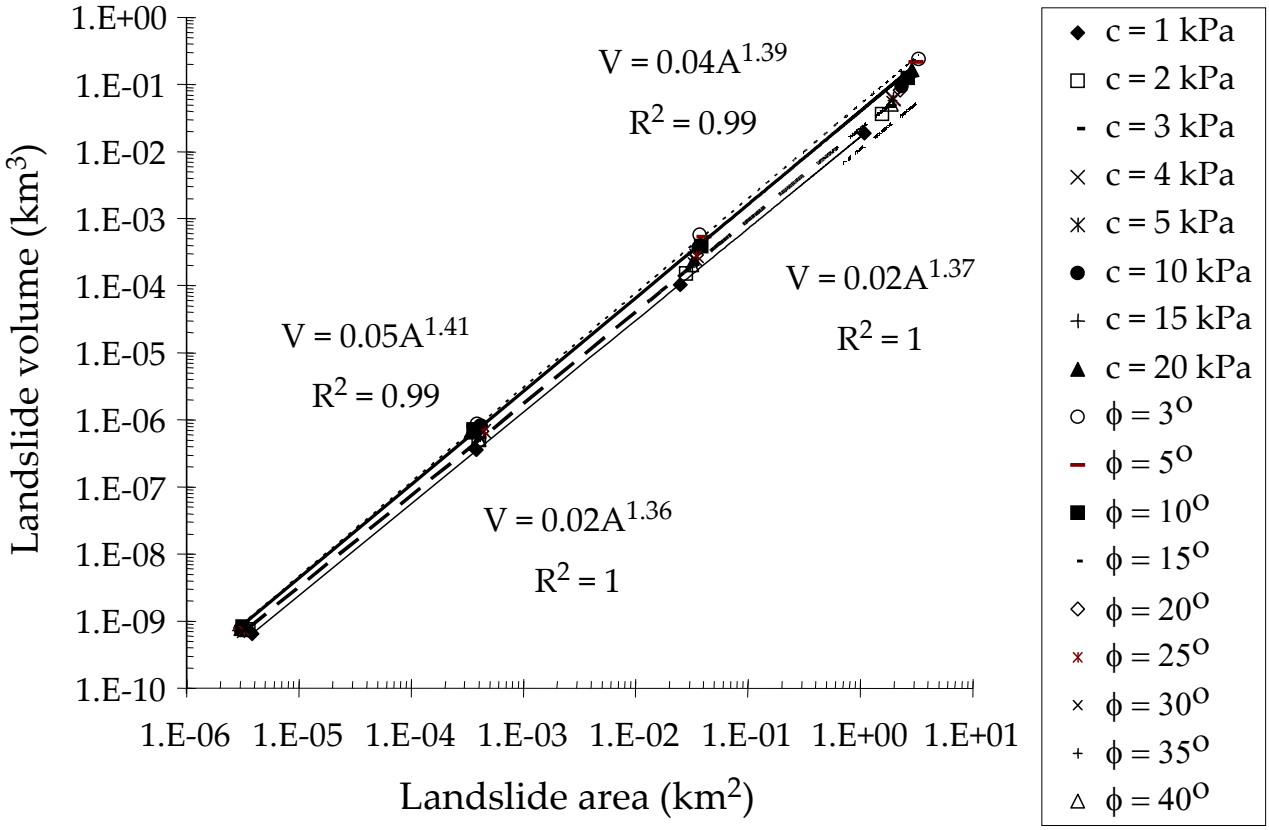

Figure 5 .Model predicted area (A) vs. volume (V) of landslides at fixed unit weight (γ = 18kN/m^3), fixed slope angle (β = 26.57°) and changing slope height (H = 1, 10, 100, 1000m). Shown here are the trend lines and regression equations of the 4 extreme cases: (a) c = 1kPa , ϕ = 25° (thin solid line); (b) c = 20kPa , ϕ = 25° (heavy solid line); (c) c = 5kPa , ϕ = 3° (dotted line); (d) c = 5kPa , ϕ = 40° (dashed line).

At~ $H^3 \sim A^{1.5}$. This would be the situation if landslides showed self-similar geometry (see Fig. 6). However, real landslides do not show self-similar geometry; instead they are self-affine (Turcotte, 1993). Self affine behavior is defined as a scaling transformation such that if length l is multiplied by c, the thickness t is multiplied by c^{α}, i.e.,

$$(3a) \quad l \rightarrow cl$$

$$(3b) \quad t \rightarrow c^{\alpha} t$$

In some texts α is called the Hurst exponent (Barabási and Stanley, 1995). We calculated the Hurst exponent for our simulations and found that the results indeed follow a self-affine behavior (to a certainty of 99% over the 4 orders of magnitude studied here), with α=0.74. This self-affine behavior leads to $V \sim A^{1.4}$, both in the field and in the model. The physics behind the observation that $V = A^{1.4}$ and not $A^{1.5}$ is important, and the difference in the power-law is not simply an error in measurement. It stems from the fact that landslides are self-affine and not self-similar. The implications for the deviation of the power from 1.5 are that as the area of landslides increases they become relatively shallower (Fig. 6). Although modeling reproduces the result of the field, the physics leading to self-affine geometry is yet to be revealed.

2. Why do different landslide types, from different locations, triggered by different mechanisms follow the same universal proportions? The answer is that the ratio of t to l on the failure plane is not very sensitive to mechanical properties, as long as the angle of internal friction (ϕ) and the cohesion (c) are greater than zero and are not exceedingly large (Fig. 4). Mechanical properties of natural landslides fall well within this range since they always occur on 'weak planes', either low-strength rock layer or bedding plane, so that ϕ and c are limited to be fairly low, but above zero. In this range of properties, the resulting differences in the proportions of failure planes are fairly insignificant.

4.1 The ratio between landslide thickness and area

Hovius et al. (1997), defines a ratio, ε, between landslide thickness (t) and 1D surface dimension: l (~$\sqrt{A}$):

$$(4) \quad \varepsilon = t / l$$

Figure 6. Self-similar and self-affine landslide geometry. Landslides I and III are self-similar (i.e., t and l of landslide I are increased by a factor of three to form landslide III). Landslides I and II are self-affined (i.e., l is increased by a factor of three and t is calculated according to Eq. 3b with b = 3 and a = 0.74).

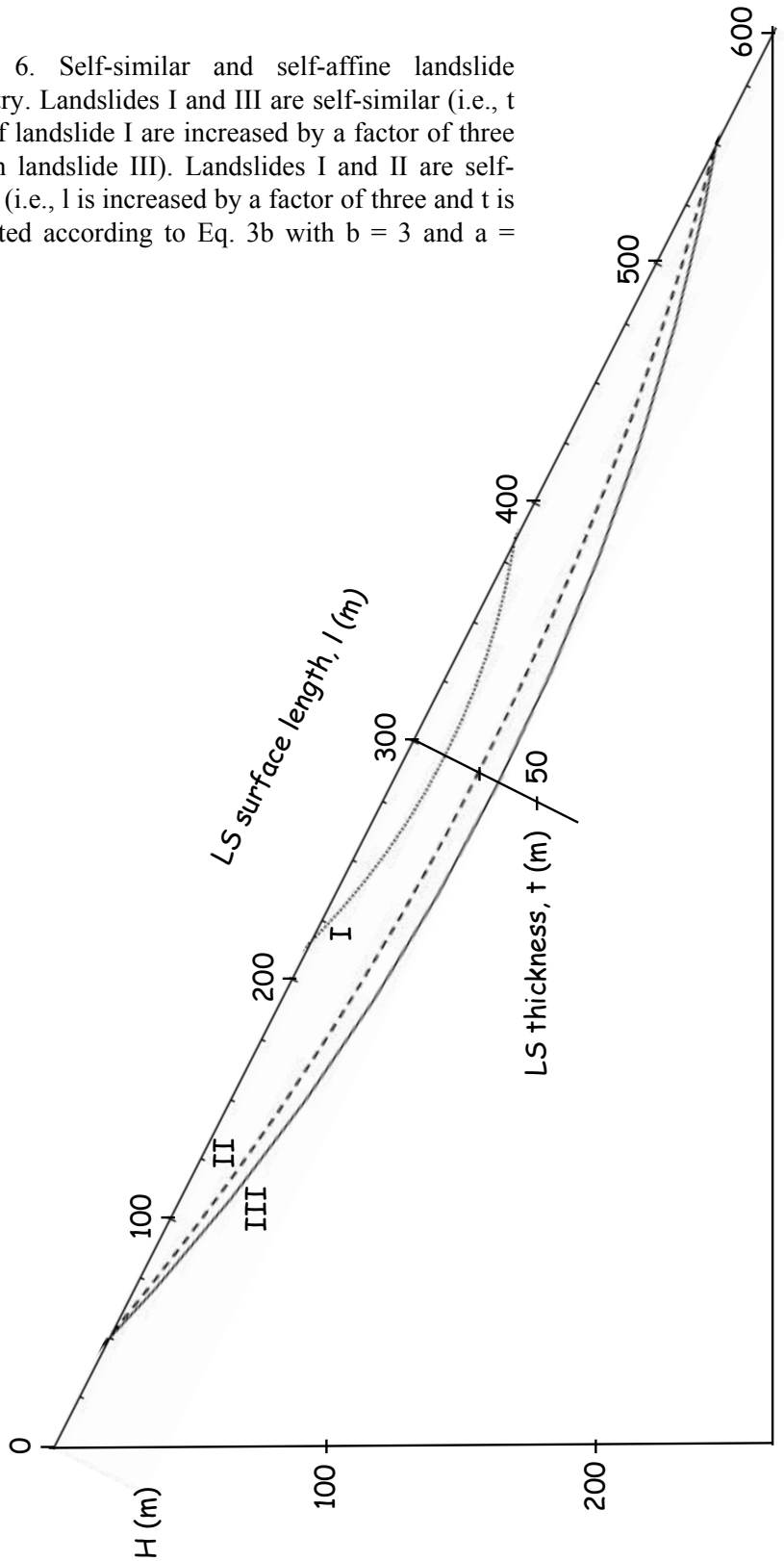

Using field observations they found that ε is roughly constant with a value of 0.05±0.02. The assumption that ε is constant implies that landslides are self-similar i.e., when stretched in one direction they are stretched by the same factor in the other direction. However, both the model and field observations with a wide range of landslide area (Hovius et al. investigated three orders of magnitude while our data spans seven orders of magnitude) imply that landslides are not self similar (i.e.. do not follow $V \sim A^{1.5}$). Instead we find that landslides are self-affine with a Hurst exponent $\alpha = 0.74$. This result implies (Fig. 7) that ε changes with the scale and from the definition of self-affinity (Eq. 3) and Equation 4 must follow

$$\varepsilon \sim l^d \sim A^{d/2} \qquad (5)$$

with $d = \alpha - 1 = -0.26$. Figure 7 plots the calculated ε vs. calculated A in our model. Figure 7 shows a power-law relation between A and ε with a power of -0.12. This power law fits the prediction of Eq. (5). Thus, ε decreases weakly with increasing landslide area as (Fig. 7):

$$\varepsilon \sim A^{-0.13} \qquad (6)$$

We believe the reason that Hovius et al. (1997), concluded that ε is constant is that their observational range was for slides of areas between 10^{-3} – 1 km^2 (Fig. 2 of Hovius et al., 1997). Our model investigates a larger range of slide areas, and indeed is close to the observation of Hovius that $\varepsilon = 0.05 \pm 0.02$ within their range of slide areas studied. Using a constant ε is an approximation that holds well within a large range, but an accurate prediction for ε is obtained from Eq. 6.

4.2. Implications for hazard analysis

It is interesting that our modeling results, obtained using a homogenous model, agree perfectly with the field data that originates from an obviously heterogeneous environment, with widely ranging mechanical properties. This agreement can be attributed to the very weak dependence that model landslide geometry shows on mechanical properties. Thus we suggest that although modeling in heterogeneous environments must still be done, tentative conclusions regarding natural landslide geometry may be drawn already from these initial results. An important conclusion is the universal relation between thickness and area of landslides. This relation can be used for hazard analysis.

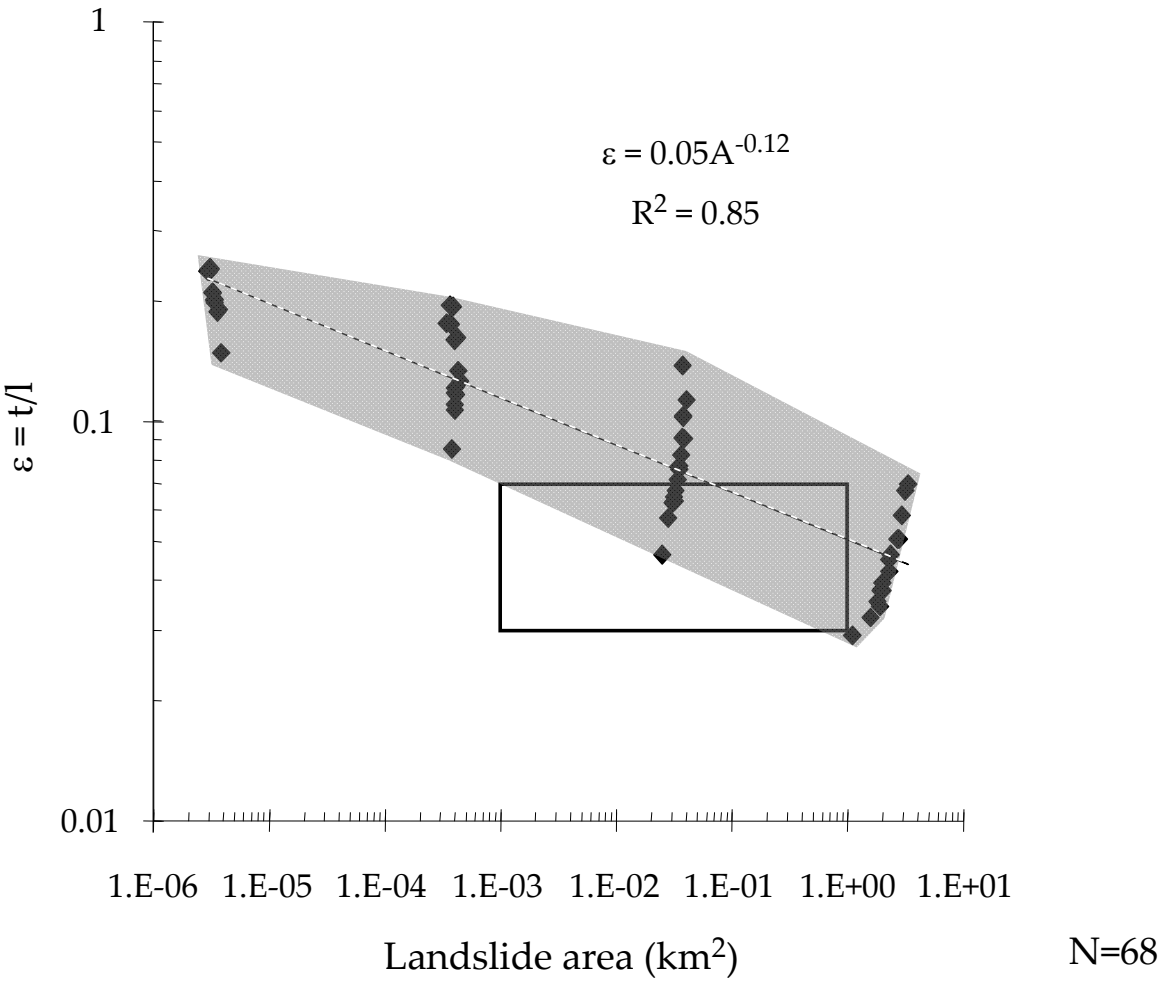

Figure 7. The ratio e (between landslide thickness, t, and landslide surface length, l) as a function of the landslide area, A. Diamonds are simulation results, where their range spans the range of mechanical properties used in modeling; the dashed line is the power-law regression for all our simulation results; the gray polygon is plotted so as to cover the data range, suggesting the expected range of e. The bold-line rectangle represents the range of observed landslide areas and e according to Hovius et al., 1997 (their fig. 2).

There are two major implications to hazard analysis. First, using the modeled and field validated relation between V and A, we obtained the full relation between t and A. These relationship can be used to predict an expected landslide area given a depth of a potential failure surface (e.g., a clay layer), t, which is calculated by slope stability analysis. As far as we know this is the first attempt to evaluate expected landslide dimensions of a studied slope. Second, for landslide induced tsunami hazard, the landslide volume (V) is the major controlling factor on tsunami wave height (Løvholt et al., 2005; Haugen et al., 2005; Vanneste et al., 2006). Generally, the available data for submarine landslide identification is a bathymetric map from which only the landslide area (A) can be estimated. The volume of a landslide is often only an estimation, for example, by fitting a smooth surface over a three-dimensional scarp (ten Brink et al., 2006) or based on the approximate extent of large, pronounced morphological structures, etc. (e.g., Løvholt et al., 2005). Using our V to A relation, the volume of a landslide, which is a significant parameter for landslide-induced tsunami modeling (e.g., ten Brink *et al.*, 2006) can now be more precisely evaluated.

5. Conclusions

Based on computer simulations, a universal relationship between volume and area of landslides has been established. This relationship follows a power law ($V \sim A^{1.4}$) and is nearly independent of slope height and mechanical properties. The power law has a similar exponent as that for the distribution of both natural subaerial and submarine landslides, despite differences in scale and processes. This volume distribution can be applied to estimate the expected size of a landslide, given the soil thickness or potential failure plane (dictates t), and to estimate the hazard of landslide-generated tsunamis.

6. Acknowledgments

This work was funded by the Steering Committee for Preparation for Earthquakes

7. Reference

Abele, G. (1974). Bergsturze in den Alpen – ihre Verbreitung, Morphologie und Folgeerscheinungen, Wiss. Alpenvereinshefte, 25, 247 p.

Barabási, A.L., Stanley, H.E., 1995. Fractal Concepts in Surface Growth. Cambridge University Press, Cambridge.

Bishop, A.W., 1955. The use of the slip circle in the stability analysis of slopes. Geotechnique, 5 (1), 7-17.

Guzzetti, F., Ardizzone, F., Cardinali, M., Galli, M., Reichenbach, P., Rossi M. 2008. Distribution of landslides in the Upper Tiber River basin, central Italy. Geomorphology, 96, 105-122.

Haugen K.B., Løvholt F., Harbitz C.B., (2005). Fundamental mechanisms for tsunami generation by submarine mass flows in idealized geometries. Marine and Petroleum Geology, 22, 209-217.

Hovius, N., Stark, C.P., Allen, P.A., 1997. Sediment flux from a mountain belt derived by landslide mapping, Geology, 25, 231–234.

Korup, O., 2006. Effects of large deep-seated landslides on hillslope morphology, western Southern Alps, New Zealand. Journal of Geophysical Research 11, F01018, doi.10.1029/2004JF000242.

Løvholt F., Harbitz C.B., Haugen K.B., (2005). A parametric study of tsunamis generated by submarine slides in the Ormen Lange/Storegga area off western Norway. Marine and Petroleum Geology, 22, 219-231.

Scholz, C.H., 2002. The Mechanics of Earthquakes and Faulting (2nd Edition). Cambridge University Press, 471 p.

Simonett, D.S., 1967. Landslide distribution and earthquakes in the Bewani and Torricelli mountains, New Guinea. In: Jennings, J. N., Mabbutt, J. A. (eds), Landform Studies from Australia and New Guinea. Cambridge University Press, Cambridge, pp. 64-84.

ten Brink, U.S., Geist, E.L., Andrews, D. 2006. Size distribution of submarine landslides and its implication to tsunami hazard in Puerto Rico. Geophysical Research Letters 33, L11307, doi.10.1029/2006GL026125.

Turcotte, D.L., 1993. Fractals and Chaos in Geology and Geophysics. Cambridge University Press, 221 p.

Vanneste M., Mienert J., Bünz, S., (2006). The Hinlopen Slide: A giant, submarine slope failure on the northern Svalbard margin, Arctic Ocean. EPSL, 245, 373-388.

Whitehouse, I.E., 1983. Distribution of large rock avalanche deposits in central Southern Alps New Zealand. N. Z. J. Geol. Geophys. 26, 272-279.

Whitehouse, I.E., 1986. Geomorphology of a compressional plate boundary, Southern Alps New Zealand, in International Geomorphology, edited by V. Gardiner, John Wiley, Hoboken, N. J., pp 897-924.

משרד התשתיות הלאומיות
המכון הגיאולוגי

ניתוח היחס בין נפח ושטח של גלישות מדרון;
במסגרת הערכת הסכנה לצונאמי תוצר גלישה במדרון-
היבשת בחוף הים התיכון הישראלי

בוריאנה קלדרון-עשהאל, עודד כץ, עינת אהרונוב, שמואל מרקו

מוגש לועדת ההיגוי
להיערכות וטיפול ברעידות אדמה

דוח מס׳ GSI/06/2008 ירושלים, ניסן תשס״ח, אפריל 2008